

More on the regularized big bang singularity

F.R. Klinkhamer*

*Institute for Theoretical Physics,
Karlsruhe Institute of Technology (KIT),
76128 Karlsruhe, Germany*

Abstract

The big bang singularity of the expanding-universe Friedmann solution of the Einstein gravitational field equation can be regularized by the introduction of a degenerate metric and a nonzero length scale b . The result is a nonsingular bounce of the cosmic scale factor with a contracting prebounce phase and an expanding postbounce phase. The corresponding maximum values of the curvature and the energy density occur at the moment of the bounce and are proportional to powers of $1/b$. This article presents a detailed calculation of the dynamics of such a nonsingular bounce. In addition, a comparison is made between this nonsingular bounce and the bounces of loop quantum cosmology and string cosmology.

PACS numbers: 04.20.Cv, 98.80.Bp, 98.80.Jk

Keywords: general relativity, big bang theory, mathematical and relativistic aspects of cosmology

* frans.klinkhamer@kit.edu

I. INTRODUCTION

The Friedmann solution [1–3] of Einstein’s gravitational field equation describes an expanding universe, assumed to be homogeneous and isotropic. The big bang singularity of the Friedmann solution can be regularized [4] by the introduction of a degenerate metric with a vanishing determinant on a three-dimensional submanifold of spacetime and a nonzero length scale b . The original big bang singularity [at cosmic time coordinate $t = t_{\text{bb}}$ with vanishing cosmic scale factor $a(t_{\text{bb}}) = 0$] is replaced by a three-dimensional “defect” of spacetime [the defect occurs at cosmic time coordinate $T = T_B$ and has a cosmic scale factor $a(T_B) \neq 0$, for a new coordinate T that is defined later].

The interpretation of the degenerate metric in Ref. [4] as corresponding to a spacetime defect [5, 6] is recalled below. At this moment, we only mention that we consider general relativity, albeit in an extended version that allows for degenerate metrics (see the last two paragraphs of Sec. I in Ref. [4] for further details).

Three follow-up papers [7–9] of the regularized-big-bang paper [4] discuss certain phenomenological aspects of the resulting nonsingular bouncing cosmology. See Ref. [10] for a review of the basic ideas of nonsingular bouncing cosmology and an extensive list of references.

The calculations of the follow-up papers [7, 8], in particular, use an auxiliary cosmic time coordinate $\tau = \tau(T)$, for which the reduced field equations are nonsingular and, therefore, directly accessible to numerical analysis. These reduced field equations are, in fact, ordinary differential equations (ODEs) and may be called the τ -ODEs. But the auxiliary coordinate τ differs essentially from the cosmic time coordinate T that enters the metric. The corresponding reduced field equations in terms of T are singular ODEs and precisely the singularities in these T -ODEs force the solution $a(T)$ to be nonsingular, with a nonzero cosmic scale factor $a(T_B) \neq 0$ at the moment of the cosmic bounce, $T = T_B$.

The goal of the present article is to carefully study these singular T -ODEs, in order to understand the dynamics of the time-symmetric nonsingular bounce. The outline is as follows. In Sec. II, we recall the *Ansatz* for the metric from Ref. [4], and discuss an advantage and a disadvantage of this *Ansatz*. In Sec. III, we present a new *Ansatz* for the metric, which may or may not have a bounce, depending on the dynamics. In Sec. IV, we obtain analytic and numerical results for this new metric with appropriate boundary conditions at the bounce, where the main focus is on establishing the smooth behavior of physical quantities at the bounce. In Sec. V, we expand on the subtle issue of boundary

conditions (a calculation with initial conditions is presented in Appendix A). In Appendix B, we compare our degenerate-metric bounce with the bounces of loop quantum cosmology and string cosmology.

II. FIRST METRIC ANSATZ

For a modified spatially flat Friedmann–Lemaître–Robertson–Walker (FLRW) universe with cosmic time coordinate T and comoving spatial Cartesian coordinates $\{X^1, X^2, X^3\}$, a relatively simple *Ansatz* of a degenerate metric is given by [4]

$$ds^2 \Big|^{(\text{type-1})} \equiv g_{\mu\nu}(X) dX^\mu dX^\nu \Big|^{(\text{type-1})} = -\frac{T^2}{T^2 + b^2} dT^2 + \tilde{a}^2(T) \delta_{kl} dX^k dX^l, \quad (2.1a)$$

$$b^2 > 0, \quad (2.1b)$$

$$\tilde{a}(T) \in \mathbb{R}, \quad (2.1c)$$

$$T \in (-\infty, \infty), \quad X^k \in (-\infty, \infty), \quad (2.1d)$$

where $b > 0$ corresponds to the length scale of a spacetime defect (cf. Refs. [5, 6] and references therein). For definiteness, we call this previous metric (2.1a) the “type-1” metric. The metric from (2.1a) is degenerate, having $\det g_{\mu\nu} = 0$ at $T = 0$. We remark that the spacetime resulting from the metric (2.1) is no longer independent of the choice of foliation [11, 12], as the hypersurface $T = 0$ is singled out. Incidentally, this degeneracy hypersurface can be shifted to $T = T_B$ by replacing the metric component g_{00} in (2.1a) by $-(T - T_B)^2 / ((T - T_B)^2 + b^2)$.

We assume that the matter content is described by a homogeneous perfect fluid with energy density $\rho_M(T)$ and pressure $P_M(T)$. From the Einstein gravitational field equation [2] and the metric (2.1a), we then obtain the dynamic equations for the variables $\tilde{a}(T)$, $\rho_M(T)$, and $P_M(T)$. These equations are the energy-conservation equation of the matter, the equation of state relating $P_M(T)$ to $\rho_M(T)$, the modified first-order spatially flat Friedmann equation, and the modified second-order spatially flat Friedmann equation:

$$\rho'_M + 3 \frac{\tilde{a}'}{\tilde{a}} [\rho_M + P_M] = 0, \quad (2.2a)$$

$$P_M = P_M(\rho_M), \quad (2.2b)$$

$$\left[1 + \frac{b^2}{T^2}\right] \left(\frac{\tilde{a}'}{\tilde{a}}\right)^2 = \frac{8\pi G_N}{3} \rho_M, \quad (2.2c)$$

$$\left[1 + \frac{b^2}{T^2}\right] \left(\frac{\tilde{a}''}{\tilde{a}} + \frac{1}{2} \left(\frac{\tilde{a}'}{\tilde{a}}\right)^2\right) - \frac{b^2}{T^3} \frac{\tilde{a}'}{\tilde{a}} = -4\pi G_N P_M, \quad (2.2d)$$

where the prime stands for differentiation with respect to T .

The ODEs (2.2c) and (2.2d) reproduce, in the formal limit $b \rightarrow 0$, the standard Friedmann equations [2]. The modified Friedmann equations (2.2c) and (2.2d) can, in fact, be rewritten as the standard Friedmann equations with an additional effective energy density ρ_{defect} and an additional effective pressure P_{defect} , both proportional to $-b^2/(b^2 + T^2)$. For a bounce solution [4] with finite values of ρ_M and P_M at the moment of the bounce ($T = 0$), the total effective energy density $\rho_{\text{total}} \equiv \rho_M + \rho_{\text{defect}}$ and the total effective pressure $P_{\text{total}} \equiv P_M + P_{\text{defect}}$ violate the Null Energy Condition over a finite time interval I_B around $T = 0$: $[\rho_{\text{total}} + P_{\text{total}}]_{T \in I_B} < 0$. We remark also that, if $\tilde{a}'(T)/\tilde{a}(T)$ were to vanish at a cosmic time $T = T_{\text{stop}} \neq 0$, this would require a vanishing matter energy density, $\rho_M(T_{\text{stop}}) = 0$, according to (2.2c).

The advantage of the metric (2.1a) is that it takes the standard FLRW form,

$$ds^2 \Big|_{(\text{type-1, } \tau\text{-coord.})} = -d\tau^2 + \hat{a}^2(\tau) \delta_{kl} dX^k dX^l, \quad (2.3)$$

if we replace the coordinate T by the coordinate τ , which is defined as follows:

$$\tau(T) = \begin{cases} +\sqrt{b^2 + T^2}, & \text{for } T \geq 0, \\ -\sqrt{b^2 + T^2}, & \text{for } T \leq 0, \end{cases} \quad (2.4)$$

where $\tau = -b$ and $\tau = b$ correspond to the single point $T = 0$ on the cosmic time axis. The coordinate transformation (2.4) is noninvertible (two different τ values for the single value $T = 0$) and is not a diffeomorphism. This implies that the differential structure of the spacetime manifold with metric (2.1a) differs from the differential structure of the spacetime manifold with metric (2.3); see Ref. [6] for an extensive discussion. For practical calculations [7–9], the metric (2.3) is to be preferred, as that metric is relatively simple and the corresponding τ -ODEs nonsingular.

But, with the different differential structure from (2.1a) and (2.3), the actual study of the bounce at $T = 0$ requires the T -ODEs (2.2). The disadvantage of the metric *Ansatz* (2.1a), then, is that it explicitly depends on the coordinate T , as do the corresponding ODEs (2.2c) and (2.2d). It would be preferable to have a metric that depends only on the scale factor and its derivatives. Another desirable property of this new metric would be that the appearance of a bounce is not hardwired into the metric *Ansatz* but that the bounce occurs dynamically.

III. SECOND METRIC ANSATZ

We now present another metric *Ansatz* for a modified spatially flat FLRW universe, with the metric depending only on the scale factor and its derivatives, apart from two constants (b and a_B). For definiteness, we call this new metric the “type-2” metric. Specifically, the new metric reads

$$ds^2 \Big|^{(\text{type-2})} = -\frac{[a(T) - a_B]^2}{[a(T) - a_B]^2 + b^2 [a'(T)/2]^2} dT^2 + a^2(T) \delta_{kl} dX^k dX^l, \quad (3.1a)$$

$$b^2 > 0, \quad (3.1b)$$

$$a_B > 0, \quad (3.1c)$$

$$a(T) \in \mathbb{R}, \quad (3.1d)$$

$$T \in (-\infty, \infty), \quad X^k \in (-\infty, \infty), \quad (3.1e)$$

where the prime stands, again, for differentiation with respect to T . With the metric (3.1), a bounce occurs at $T = T_B$ if

$$a(T_B) = a_B, \quad (3.2a)$$

$$a'(T_B) = 0. \quad (3.2b)$$

Whether or not the conditions (3.2) are fulfilled depends on the dynamics and the boundary conditions (see below). An explicit realization of the bounce behavior is given by

$$a(T) \sim a_B + c_2 (T - T_B)^2, \quad (3.3)$$

for a nonzero constant c_2 .

We observe that close to a bounce, with $a(T) \sim a_B + c_2 T^2$ for $T_B = 0$ and $c_2 \neq 0$, the g_{00} component from (3.1a) reduces to the expression $-T^4/(T^4 + b^2 T^2)$, which has essentially the same structure as the g_{00} component of the type-1 metric (2.1a). In principle, it is also possible to consider a metric *Ansatz* without explicit mention of a_B (an example would be $g_{00} = -(a')^2/[(a')^2 + b^2 (a'')^2]$), but the *Ansatz* (3.1a) suffices for the purpose of studying the bounce dynamics. Note that the type-2 metric *Ansatz* (3.1) differs from the type-1 metric *Ansatz* (2.1) because, with the respective dynamic equations, the type-2 metric may or may not have a bounce, whereas the type-1 metric always has a bounce at $T = 0$, as long as $\rho_M > 0$ (see Appendix A 2 for a direct comparison of the two metrics).

Just as in Sec. II, we assume that the matter content is given by a homogeneous perfect fluid. From the Einstein gravitational field equation [2] and the new metric (3.1a), we then obtain the dynamic equations for the variables $a(T)$, $\rho_M(T)$, and $P_M(T)$. These equations are the energy-conservation equation of the matter, the equation of state of the matter, the (new) modified first-order spatially flat Friedmann equation, and the (new) modified second-order spatially flat Friedmann equation:

$$\rho'_M + 3 \frac{a'}{a} [\rho_M + P_M] = 0, \quad (3.4a)$$

$$P_M = P_M(\rho_M), \quad (3.4b)$$

$$\left[1 + \frac{b^2}{4} \frac{a^2}{[a - a_B]^2} \left(\frac{a'}{a} \right)^2 \right] \left(\frac{a'}{a} \right)^2 = \frac{8\pi G_N}{3} \rho_M, \quad (3.4c)$$

$$\left[1 + \frac{1}{2} \frac{b^2 [a']^2}{[a - a_B]^2} \right] \frac{a''}{a} + \frac{1}{2} \left(\frac{a'}{a} \right)^2 + \frac{1}{8} b^2 \frac{a^2 [a + a_B]}{[a - a_B]^3} \left(\frac{a'}{a} \right)^4 = -4\pi G_N P_M. \quad (3.4d)$$

We have the following remarks:

1. The ODEs (3.4c) and (3.4d) reproduce, in the formal limit $b \rightarrow 0$, the standard Friedmann equations [2].
2. Precisely the b^2 terms of the ODEs (3.4c) and (3.4d) contain various powers of the factor $a'(T)/[a(T) - a_B]$, which is singular at $T = T_B$ for $a(T)$ from (3.3).
3. The singular b^2 term in (3.4c) allows for a nontrivial bounce solution at $T = T_B$, with $a(T)$ from (3.3) and $\rho_M(T) \sim r_0 + r_2(T - T_B)^2$ for positive a_B and r_0 ; see Sec. IV A for further details.
4. If $a'(T)$ were to vanish at a cosmic time $T = T_{\text{stop}} \neq T_B$ with $a(T_{\text{stop}}) \neq 0$ and $a(T_{\text{stop}}) \neq a_B$, this would require a vanishing energy density, $\rho_M(T_{\text{stop}}) = 0$, according to (3.4c).
5. It can be verified that the second-order ODE (3.4d) follows from the first-order ODEs (3.4a) and (3.4c); see the discussion in Sec. 15.1 of Ref. [2] for the case of the standard Friedmann equations.
6. The ODEs (3.4a), (3.4c), and (3.4d) are invariant under the rescaling $a(T) \rightarrow \zeta a(T)$ and $a_B \rightarrow \zeta a_B$ for $\zeta \in \mathbb{R} \setminus \{0\}$, and also under time reversal $(T - T_B) \rightarrow -(T - T_B)$ if a , ρ_M , and P_M are even functions of $T - T_B$.

From now on, we assume that the matter content is described by a homogeneous perfect fluid with a *constant* equation-of-state parameter,

$$W_M(T) \equiv P_M(T)/\rho_M(T) = w_M = \text{constant} . \quad (3.5)$$

Furthermore, we use reduced-Planckian units, with

$$8\pi G_N = c = \hbar = 1 , \quad (3.6)$$

and take the following model parameters:

$$b = 1 , \quad (3.7a)$$

$$w_M = 1 , \quad (3.7b)$$

where this particular choice for w_M aims at avoiding instabilities in the prebounce phase (see, e.g., Sec. IV of Ref. [10] and references therein). In order to compare with previous results, we choose the following value for the bounce scale factor in (3.1) and (3.4)

$$a_B = 1 , \quad (3.8a)$$

and take the following value for the bounce time

$$T_B = 0 , \quad (3.8b)$$

but the value of a_B can be arbitrarily rescaled and the value of T_B can be arbitrarily shifted.

IV. BOUNCE SOLUTION WITH BOUNDARY CONDITIONS AT THE BOUNCE

In this section, we discuss the solution of the ODEs (3.4) with appropriate boundary conditions at the bounce. Specifically, we take the following boundary conditions:

$$a(0) = 1 , \quad (4.1a)$$

$$a'(0) = 0 , \quad (4.1b)$$

$$\rho_M(0) > 0 , \quad (4.1c)$$

where we have used the values $T_B = 0$ and $a_B = 1$ from (3.8).

In Sec. V, we give a general discussion of the issue of boundary conditions and, in Appendix A, we obtain solutions with initial conditions, which may or may not result in a bounce solution.

A. Analytic results

We start from the analytic solution [2] of (3.4a) for the case of a constant equation-of-state parameter w_M as defined by (3.5)

$$\rho_M(a) = r_0 a^{-3[1+w_M]}, \quad (4.2a)$$

$$r_0 > 0, \quad (4.2b)$$

where $a(T)$ is assumed to be positive and to have boundary conditions (4.1). The resulting ODEs (3.4c) and (3.4d) near $T = T_B = 0$ are approximately solved by a truncated power series,

$$a(T) = 1 + \sum_{n=1}^N a_{2n} (T/b)^{2n}, \quad (4.3)$$

for appropriate values of the coefficients a_{2n} . With $N = 4$, we obtain the following coefficients (taking the positive root for a_2):

$$a_2 = \frac{1}{2\sqrt{3}} b \sqrt{r_0}, \quad (4.4a)$$

$$a_4 = -\frac{1}{72\sqrt{3}} \left(6b\sqrt{r_0} + \sqrt{3}b^2 r_0 [1 + 3w_M] \right), \quad (4.4b)$$

$$a_6 = \frac{1}{25920} b \sqrt{r_0} \left(156\sqrt{3} + 48b\sqrt{r_0} [1 + 3w_M] + \sqrt{3}b^2 r_0 [31 + 132w_M + 117w_M^2] \right), \quad (4.4c)$$

$$a_8 = -\frac{1}{362880\sqrt{3}} b \sqrt{r_0} \left(1044 - 72\sqrt{3}b\sqrt{r_0} [1 + 3w_M] + 9b^2 r_0 [29 + 120w_M + 99w_M^2] \right. \\ \left. + 2\sqrt{3}b^3 r_0^{3/2} [77 + 405w_M + 621w_M^2 + 297w_M^3] \right), \quad (4.4d)$$

where r_0 in the expressions (4.4) corresponds to $8\pi G_N \rho_0$ with mass dimension 2, so that $b\sqrt{r_0}$ is dimensionless. For $b = 1$, $w_M = 1$, and $r_0 = 1/3$, we have the following numerical values:

$$\{a_2, a_4, a_6, a_8\} \Big|_{b=1, w_M=1, r_0=1/3} \approx \{0.166667, -0.0462963, 0.0120885, -0.0022352\}, \quad (4.5)$$

which suggests an alternating series with a finite radius of convergence.

Returning to the a_2 solution (4.4a), the relevant equation is the series expansion of the modified first-order spatially flat Friedmann equation (3.4c), which reads

$$0 = 4(a_2)^2/b^2 - r_0/3 + O(T^2), \quad (4.6)$$

for $8\pi G_N = 1$ and $r_0 > 0$. As said, we have chosen the positive root for a_2 and postpone further discussion to Sec. V.

The Ricci curvature scalar $R(x) \equiv g^{\nu\sigma}(x) g^{\mu\rho}(x) R_{\mu\nu\rho\sigma}(x)$ and the Kretschmann curvature scalar $K(x) \equiv R^{\mu\nu\rho\sigma}(x) R_{\mu\nu\rho\sigma}(x)$ are readily evaluated for the metric (3.1a). The resulting expressions are functionals of the *Ansatz* function $a(T)$ and its derivatives. Inserting the truncated power series (4.3), we obtain

$$R(T) = \frac{1}{b^2} \sum_{n=0}^{N'} R_{2n} (T/b)^{2n}, \quad (4.7)$$

$$K(T) = \frac{1}{b^4} \sum_{n=0}^{N''} K_{2n} (T/b)^{2n}. \quad (4.8)$$

With the a -coefficients from (4.4), we get

$$R_0 = b^2 r_0 (1 - 3 w_M), \quad (4.9a)$$

$$R_2 = -\frac{1}{2} \sqrt{3} b^3 r_0^{3/2} (1 - 2 w_M - 3 w_M^2), \quad (4.9b)$$

$$R_4 = \frac{1}{24} b^3 r_0^{3/2} (1 - 2 w_M - 3 w_M^2) \left(2\sqrt{3} + b\sqrt{r_0} [13 + 12 w_M] \right), \quad (4.9c)$$

and

$$K_0 = \frac{1}{3} b^4 r_0^2 (5 + 6 w_M + 9 w_M^2), \quad (4.10a)$$

$$K_2 = -\frac{1}{\sqrt{3}} b^5 r_0^{5/2} (5 + 11 w_M + 15 w_M^2 + 9 w_M^3), \quad (4.10b)$$

$$K_4 = \frac{1}{36} b^5 r_0^{5/2} (5 + 11 w_M + 15 w_M^2 + 9 w_M^3) \left(2\sqrt{3} + b\sqrt{r_0} [22 + 21 w_M] \right). \quad (4.10c)$$

The perturbative results (4.9) suggest that $R(T) = 0$ for the case of relativistic matter with $w_M = 1/3$, just as for the standard FLRW universe [2]. The numerical values of the coefficients (4.9) and (4.10) for $b = 1$, $w_M = 1$, and $r_0 = 1/3$ are

$$\{R_0, R_2, R_4\} \Big|_{b=1, w_M=1, r_0=1/3} \approx \{-0.666667, 0.666667, -0.574074\}, \quad (4.11a)$$

$$\{K_0, K_2, K_4\} \Big|_{b=1, w_M=1, r_0=1/3} \approx \{0.740741, -1.48148, 2.01646\}. \quad (4.11b)$$

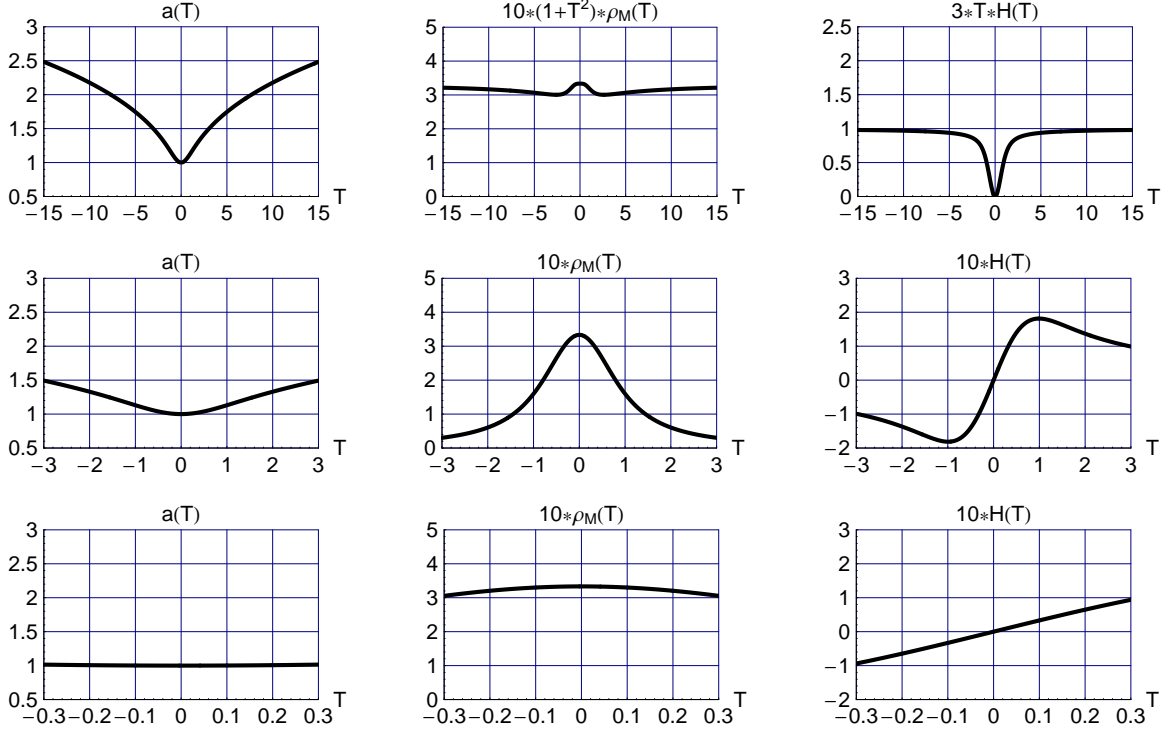


FIG. 1. Solution of the ODEs (3.4a) and (3.4c) for a constant equation-of-state parameter w_M from (3.5) and reduced-Planckian units (3.6). The model parameters are $b = 1$ and $w_M = 1$. The boundary conditions at $T = T_B = 0$ are $a(0) = a_B = 1$ and $\rho_M(0) = r_0$ for $r_0 = 1/3$. The approximate analytic solution is shown over $T \in (-\Delta T, \Delta T)$ and the numerical solution over $T \in [-T_{\max}, -\Delta T] \cup [\Delta T, T_{\max}]$, with $\Delta T = 1/10$ and $T_{\max} = 15$. Specifically, the approximate analytic solution for $a(T)$ is given by (4.3) and (4.4) for $N = 4$, while the analytic solution for $\rho_M(T)$ follows from (4.2). The numerical solution is obtained from the ODEs (3.4a) and (3.4c) with boundary conditions at $T = \pm\Delta T$ from the approximate analytic solution. Shown, on the top row, are the dynamic functions $a(T)$ and $\rho_M(T)$, together with the corresponding Hubble parameter $H(T) \equiv [da(T)/dT]/a(T)$. The middle and bottom rows zoom in on the bounce at $T = 0$. In the middle panel of the top row, $10\rho_M(T)$ is scaled by a further factor $(1 + T^2)$, in order to display the asymptotic behavior $\rho_M(T) \propto 1/T^2$ as $|T| \rightarrow \infty$. Similarly, in the right panel of the top row, $H(T)$ is scaled by a factor $3T$, in order to display the asymptotic behavior $H(T) \sim (1/3)T^{-1}$.

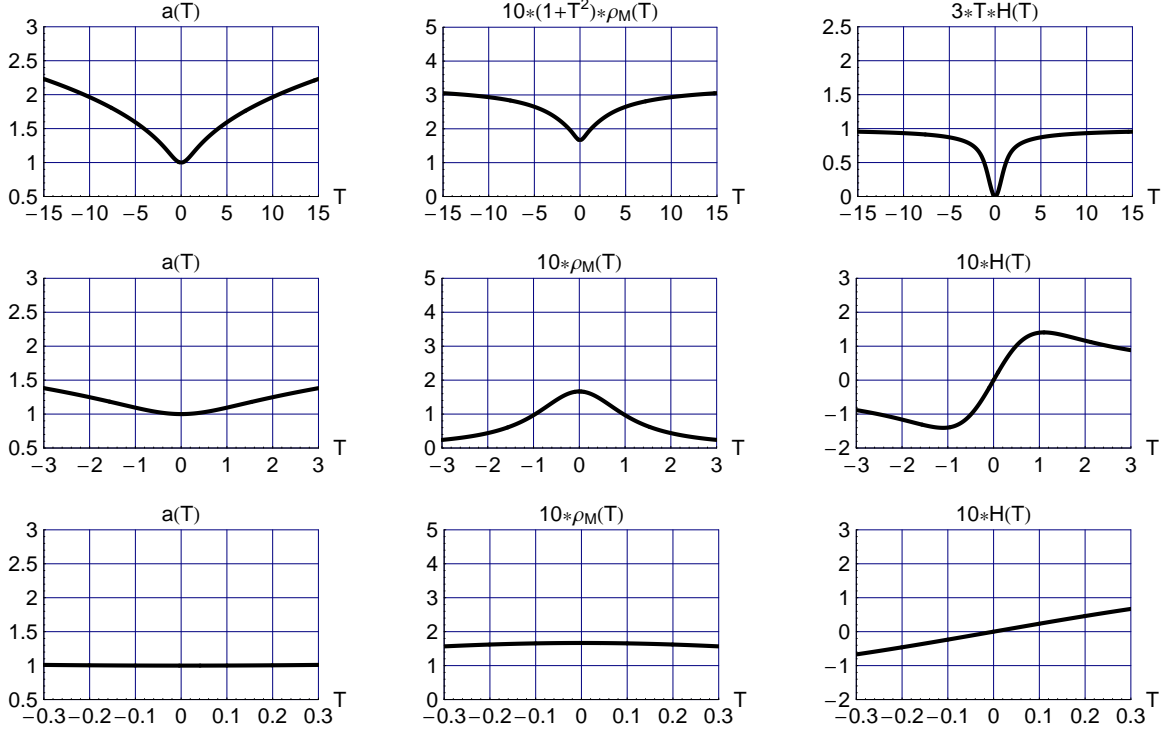


FIG. 2. Same as Fig. 1, but now with boundary condition $\rho_M(0) = r_0 = 1/6$.

For completeness, we also give the asymptotic solution for $|T| \rightarrow \infty$,

$$a_{\text{asypm}}(T) \sim a_\infty (T^2)^{p/2}, \quad (4.12a)$$

$$\rho_{M \text{ asypm}}(T) \sim r_\infty [a_{\text{asypm}}(T)]^{-3[1+w_M]}, \quad (4.12b)$$

$$a_\infty = \left(\frac{r_\infty}{3p^2} \right)^{p/2}, \quad (4.12c)$$

$$p = \frac{2}{3} \frac{1}{1+w_M}, \quad (4.12d)$$

where the constant r_∞ depends indirectly on the constant r_0 from (4.2).

In closing, we remark that we have seen that the solution $\bar{a}(T)$ of the ODEs (3.4) can be expanded perturbatively around $T = T_B = 0$. The obtained Taylor series is characterized by the numerical value of r_0 , as the values of T_B and a_B can be changed arbitrarily (here, they are taken as $T_B = 0$ and $a_B = 1$). The asymptotic solution for $a(T)$ has also been found to depend indirectly on r_0 . Similar results hold for the solution [4] from the type-1 metric of Sec. II, but, here, we have focused on the more general type-2 metric of Sec. III.

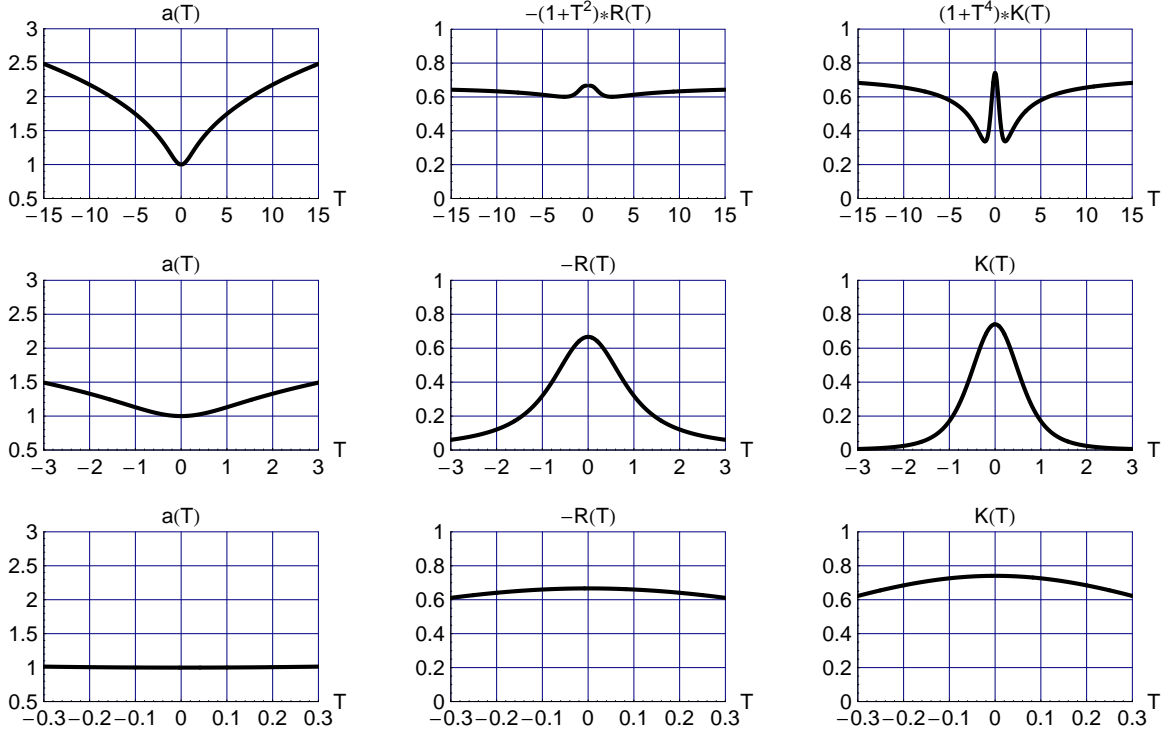


FIG. 3. Ricci curvature scalar $R(T)$ and Kretschmann curvature scalar $K(T)$ for the solution $a(T)$ of Fig. 1. In the middle panel of the top row, $-R(T)$ is scaled by a factor $(1 + T^2)$, in order to display the asymptotic behavior $-R(T) \propto 1/T^2$. Similarly, in the right panel of the top row, $K(T)$ is scaled by a factor $(1 + T^4)$, in order to display the asymptotic behavior $K(T) \propto 1/T^4$.

B. Numerical results

We obtain a close approximation of the exact solution $\bar{a}(T)$ of the ODEs (3.4), for a constant equation-of-state parameter w_M from (3.5) and with boundary conditions (4.1), by using the truncated power series (4.3) for a small enough interval around $T = T_B = 0$ and by solving the ODEs (3.4a) and (3.4c) numerically for T values outside this central interval. The ODE (3.4c) is singular at $T = 0$, if $a(0) = a_B = 1$, but this value $T = 0$ lies *outside* the intervals used for the numeric calculation. Specifically, we choose the power-series interval $[-\Delta T, \Delta T]$ and truncate the series (4.3) at $N = 4$. In principle, we must take $\Delta T \rightarrow 0$ and $N \rightarrow \infty$. We leave a detailed study of the numerical convergence properties to the future, as well as an analytic calculation (if at all possible) of the radius of convergence of the power series corresponding to (4.3). For the moment, we have just compared the results for different values of ΔT (specifically, $1/10$ or $1/100$) and different values of N (specifically, 4 or 8), and find the results to be reasonably stable.

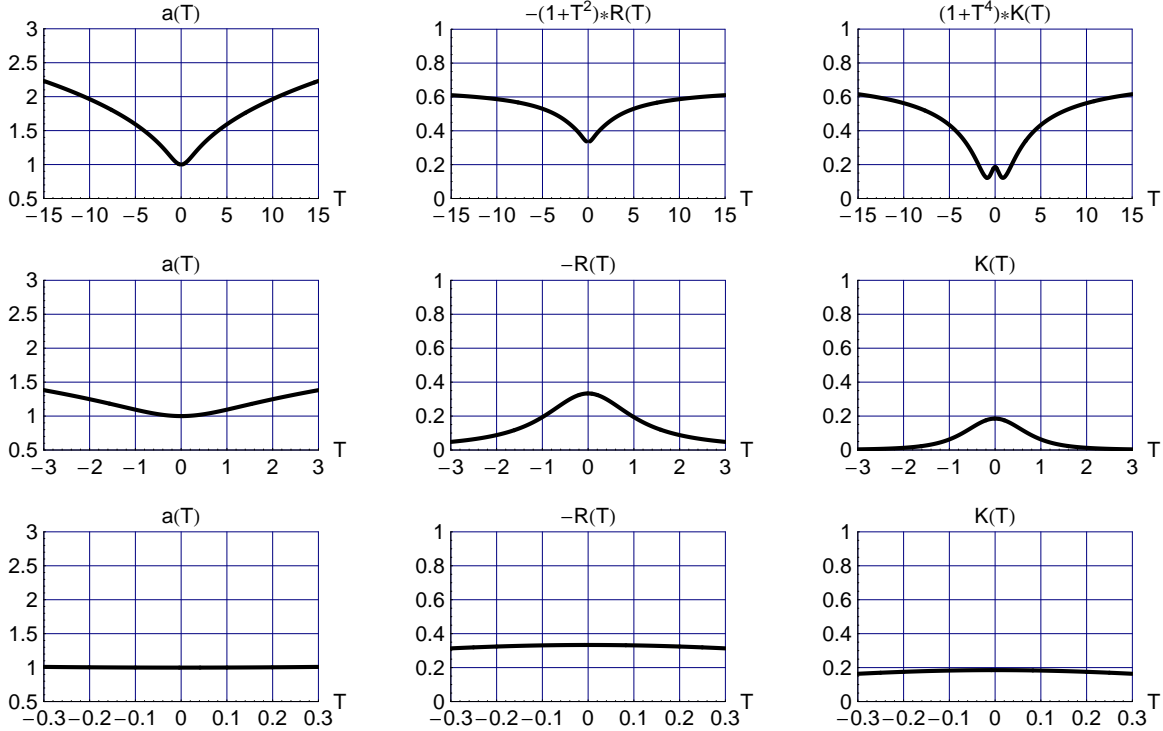


FIG. 4. Ricci curvature scalar $R(T)$ and Kretschmann curvature scalar $K(T)$ for the solution $a(T)$ of Fig. 2. The scaling of $-R(T)$ and $K(T)$ in the top-row panels is the same as used in Fig. 3.

For the numerical solution of the ODEs (3.4), we can focus on the modified first-order Friedmann ODE (3.4c). The reason is that (3.4a) already has the analytic solution (4.2a) and that, as mentioned in the fifth remark below (3.4d), the second-order Friedmann ODE (3.4d) follows from the first-order ODEs (3.4a) and (3.4c).

As to the numerical solution of the ODE (3.4c), there are two subtleties. The first subtlety is that the ODE (3.4c) is not directly accessible to numerical analysis, as the equation is quadratic in $[a']^2 \equiv S$. But we can obtain analytically the positive root of this quadratic equation for S . Then, we take the square root of S , with a minus sign of the resulting expression for a' in the prebounce phase and a plus sign in the postbounce phase. The second subtlety is that we do not numerically solve the obtained ODEs which are linear in a' (with different signs for the pre- and postbounce phases), but rather numerically solve the first derivative of these first-order ODEs. In this way, we obtain a numerical solution with a reasonably accurate value of $a''(T)$ at $T = \pm\Delta T$. In fact, we can check for the accuracy of the obtained numerical solution $a_{\text{num}}(T)$ by evaluating the residue of the second-order ODE (3.4d).

Analytic and numerical results for $b = 1$, $w_M = 1$, and $r_0 = 1/3$ are given in Fig. 1. As noted in the last paragraph of Sec. IV A, the solution is characterized by the numerical value of r_0 , for fixed values of the model parameters b and w_M . We give the results for a smaller numerical value of r_0 in Fig. 2, where the ρ_M peak is found to be lower and somewhat broader than the one in Fig. 1. The corresponding plots for the Ricci curvature scalar $R(T)$ and the Kretschmann curvature scalar $K(T)$ are given in Figs. 3 and 4.

The top-right panels in Figs. 1 and 2 show the asymptotic behavior $H(T) \sim (1/3)T^{-1}$, which results from the asymptotic behavior $a(T) \propto (T^2)^{1/6}$, as given by the analytic solution (4.12). The bottom rows in Figs. 1 and 2 illustrate the smooth behavior at the bounce $T = T_B = 0$. The smoothness of the bounce is also evident from the behavior of the Ricci curvature scalar $R(T)$ and the Kretschmann curvature scalar $K(T)$, as obtained perturbatively in (4.7) and (4.8) and shown on the bottom rows of Figs. 3 and 4,

V. DISCUSSION

We have presented, in Sec. III, a new metric *Ansatz* for a modified spatially flat FLRW universe. For the case of a constant equation-of-state parameter w_M and with appropriate boundary conditions, we have obtained, in Sec. IV, analytic results in a small interval around the cosmic time $T = T_B = 0$ of the time-symmetric bounce, together with numerical results at larger values of $|T|$ for the case of $w_M = 1$. The solution $\bar{a}(T)$ is regular at $T = 0$ and appears to be well behaved for finite values of $|T|$. The solution $\bar{a}(T)$ is characterized by the maximum energy density $\rho_M(T)$ of the matter, which occurs at $T = 0$. The dimensionless quantity for this maximum energy density is denoted r_0 , and the behavior of the analytic and numeric solutions in Figs. 1 and 2 is controlled by r_0 only, for fixed model parameters b and w_M .

As mentioned in Sec. IV A, the behavior of the $a(T)$ power series solution (4.3) near $T = T_B = 0$ has been chosen to be convex ($a_2 > 0$ with $a_B = 1$). In principle, it is also possible to have an $a(T)$ solution near $T = T_B$ that is concave ($a_2 < 0$ with $a_B = 1$), so that there will be cosmic times $T_{\pm} = T_B \pm \Delta T_{\text{bb}}$ with a vanishing scale factor, $a(T_{\pm}) = 0$. The different bounces, convex and concave at $T = T_B$, result from different initial conditions at $T_{\text{start}} < T_B$. Taking $a(T_{\text{start}}) > a_B$ and $a'(T_{\text{start}}) < 0$ gives a convex bounce, with a contracting phase for $T \in [T_{\text{start}}, T_B)$ and an expanding phase for $T \in (T_B, \infty)$. An explicit bounce solution from such initial conditions is presented in Appendix A 1. Solutions with other initial conditions are obtained in Appendix A 2, which illustrate the difference between

the metrics of Secs. II and III.

Up till now, we have not been specific as regards the numerical value of the defect length scale b , apart from the fact that this numerical value should not be too small, so as to invalidate the approximate applicability of Einstein's classical theory of gravity. In Ref. [7], we have obtained a broad range of numerical b values allowed by experiment. A hint that the defect length scale b may be close to the Planck length is obtained in Appendix B by comparing our degenerate-metric bounce with the bounce of loop quantum cosmology [13–15] (for completeness, we also compare with the bounce of string cosmology [16–19]). Moreover, it is conceptually interesting to compare our classical degenerate-metric bounce with the quantum bounce obtained from the de-Broglie-Bohm pilot-wave approach (see Ref. [20] for a review and, in particular, the discussion of Sec. 4.2.1 in that reference).

In closing, we remark that we have focused on the dynamics of a time-symmetric nonsingular bounce, with equal equation-of-state parameter w_M in the prebounce phase and the postbounce phase. But the metric (3.1a) is perfectly suited for the case of a nonsingular bounce with different values of w_M before and after the bounce. Such a time-asymmetric nonsingular bounce may be preferable for cosmological applications; see Ref. [10] and references therein. The origin of the time asymmetry may be due to a fundamental arrow of time [8] but may also be due to dissipative processes [10], or a combination of both.

ACKNOWLEDGMENTS

It is a pleasure to thank J.M. Queiruga and Z.L. Wang for comments on the manuscript and the referee for comments on an earlier version of this article.

Appendix A: Solutions from initial conditions

1. Solution with bounce

The nonsingular bounce solution in Sec. IV was obtained from boundary conditions at the moment of the bounce, $T = T_B$. Specifically, the boundary conditions of Figs. 1–4 were given at $T = T_B = 0$: $a(0) = a_B = 1$ and $\rho_M(0) = r_0$ for values $r_0 = 1/3$ or $r_0 = 1/6$. Here, we present a nonsingular bounce solution obtained from *initial* boundary conditions at $T = T_{\text{start}}$, where the actual value of T_B follows from the solution itself.

Consider the ODEs (3.4a) and (3.4c) for a constant equation-of-state parameter w_M from

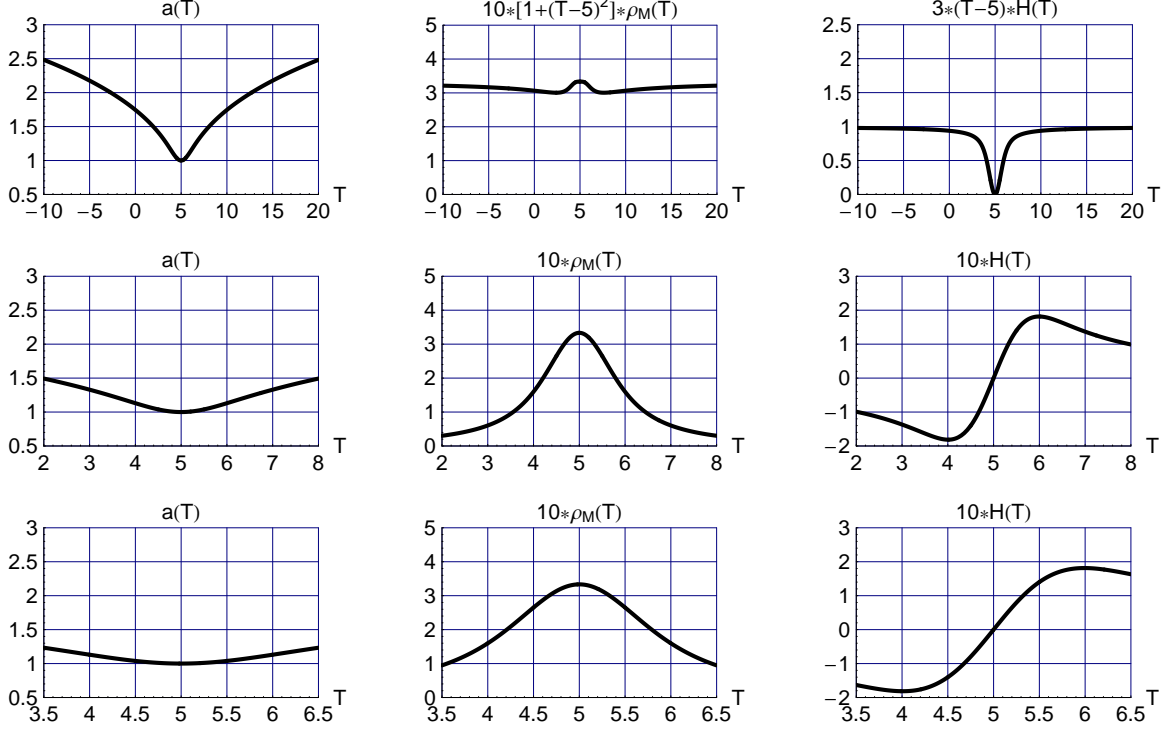


FIG. 5. Solution of the ODEs (3.4a) and (3.4c) for $a_B = 1$ and constant equation-of-state parameter w_M from (3.5). The model parameters are $b = 1$ and $w_M = 1$. Different from Fig. 1, there are now initial boundary conditions at $T = T_{\text{start}} = -10$. Specifically, the boundary conditions are $a(-10) = 2.48312$ and $\rho_M(-10)$ from (A4) for $r_0 = 1/3$ and $w_M = 1$. The numerical solution gives $T_B \approx 5.000$. In fact, the numerical prebounce solution is obtained over $T \in [-10, 5 - \Delta T]$, the analytic solution over $T \in (5 - \Delta T, 5 + \Delta T)$, and the numerical postbounce solution over $T \in [5 + \Delta T, 20]$, with $\Delta T = 1/2$. The analytic solution for $a(T)$ is given by (4.3) with $(T)^{2n}$ on the right-hand side replaced by $(T - 5)^{2n}$ and coefficients (4.5) for $N = 4$, while the analytic solution for $\rho_M(T)$ follows from (4.2). The numerical postbounce solution has boundary conditions $a(5 + \Delta T) = a(5 - \Delta T)$, $\rho_M(5 + \Delta T) = \rho_M(5 - \Delta T)$, and $a'(5 + \Delta T) > 0$. Shown, on the top row, are the dynamic functions $a(T)$ and $\rho_M(T)$, together with the corresponding Hubble parameter $H(T) \equiv [da(T)/dT]/a(T)$. The middle and bottom rows zoom in on the bounce at $T = T_B \approx 5.000$. In the middle panel of the top row, $10 \rho_M(T)$ is scaled by a further factor $[1 + (T - 5)^2]$, in order to display the asymptotic behavior $\rho_M(T) \propto 1/(T - 5)^2$ as $|T - 5| \rightarrow \infty$. Similarly, in the right panel of the top row, $H(T)$ is scaled by a factor $3(T - 5)$, in order to display the asymptotic behavior $H(T) \sim (1/3)(T - 5)^{-1}$.

(3.5) and set

$$a_B = 1. \tag{A1}$$

Next, choose an arbitrary time

$$T_{\text{start}} \in \mathbb{R}, \tag{A2}$$

at which the initial conditions are the following:

$$a(T_{\text{start}}) = a_{\text{start}} > 1, \tag{A3a}$$

$$\rho_M(T_{\text{start}}) = \rho_{M\text{-start}} > 0, \tag{A3b}$$

$$a'(T_{\text{start}}) < 0, \tag{A3c}$$

where the prime stands for differentiation with respect to T . If, for a generic value of a_{start} (with $a_{\text{start}} > 1$), the value of $\rho_{M\text{-start}}$ is chosen as

$$\rho_{M\text{-start}} = r_0 \left(a_B / a_{\text{start}} \right)^{3[1+w_M]}, \tag{A4}$$

then, for $r_0 = 1/3$ and $w_M = 1$, the bounce dynamics of Figs. 1 and 3 is reproduced, but with $T_B = 0$ shifted to a nonzero value $T_B > T_{\text{start}}$. Similarly, for $r_0 = 1/6$ and $w_M = 1$, the bounce dynamics of Figs. 2 and 4 is reproduced.

The solution from initial conditions (A3) and (A4) at $T_{\text{start}} = -10$ is shown in Fig. 5. The actual value $a_{\text{start}} = 2.48312$, for given values $r_0 = 1/3$ and $w_M = 1$ in (A4), is chosen so that the resulting value for T_B is close to $T_{\text{start}} + 15 \approx 5$, which makes the curves of Fig. 5 resemble those of Fig. 1 (with more digits in the numerical value of a_{start} , the curves of Fig. 5 become essentially identical to those of Fig. 1 with a shifted T coordinate). Different values of a_{start} (for the same values of T_{start} , r_0 , and w_M) give different values for T_B .

2. Solution without bounce

We discuss, for the case of a positive cosmological constant, a particular analytic solution of the ODEs (3.4) from the type-2 metric, and compare it to the corresponding analytic solution of the ODEs (2.2) from the type-1 metric. Even though both analytic solutions use the same type of initial conditions, their behavior is very different: the first solution does not have a bounce, whereas the second one has.

Having a positive cosmological constant Λ corresponds to setting

$$\rho_M(T) = -P_M(T) = \Lambda = \text{constant} > 0, \quad (\text{A5})$$

which trivially solves (3.4a). The remaining ODE is given by (3.4c) which reads for $a_B = 1$:

$$\left[1 + \frac{b^2}{4} \frac{a^2}{[a-1]^2} \left(\frac{a'}{a} \right)^2 \right] \left(\frac{a'}{a} \right)^2 = \frac{8\pi G_N}{3} \Lambda. \quad (\text{A6})$$

Now take the following initial conditions:

$$a(T_{\text{start}}) < 0, \quad (\text{A7a})$$

$$T_{\text{start}} < 0. \quad (\text{A7b})$$

Neglecting b , one solution of (A6) with initial conditions (A7) is simply given by

$$a(T) \Big|^{(b=0)} = -\exp[H_{\text{dS}} T], \quad (\text{A8a})$$

$$H_{\text{dS}} \equiv \sqrt{8\pi G_N \Lambda/3}. \quad (\text{A8b})$$

For small but nonzero b [specifically, $0 < (b H_{\text{dS}})^2 \ll 1$], the solution can be written as

$$a(T) = -\exp[H_{\text{dS}} f(T) T], \quad (\text{A9a})$$

with a smooth function $f(T)$ that remains close to 1 and has the following asymptotic behavior:

$$f(T) \sim \begin{cases} 1, & \text{for } T \ll -b, \\ (b H_{\text{dS}})^{-1} \left[2 \sqrt{1 + (b H_{\text{dS}})^2} - 2 \right]^{1/2}, & \text{for } T \gg b. \end{cases} \quad (\text{A9b})$$

The solution $a(T)$ from (A9) is monotonic and does not display bounce behavior at any finite value of T . Incidentally, a bounce solution does occur if, for example, the initial condition (A7a) is replaced by $a(T_{\text{start}}) > 1$: with negative a'/a at $T = T_{\text{start}}$, the solution has a bounce at $T_B > T_{\text{start}}$ and qualitatively resembles the solution found in Appendix A 1, whereas, with positive a'/a at $T = T_{\text{start}}$, the solution has a bounce at $T_B < T_{\text{start}}$.

Returning to the solution (A9) with initial conditions (A7), the corresponding solution for the type-1 metric (2.1) has been discussed in Appendix B of Ref. [4]. With similar initial conditions, $\tilde{a}(T_{\text{start}}) < 0$ for $T_{\text{start}} < 0$, such a solution of the ODE (2.2c) with $\rho_M = \Lambda > 0$ is given by

$$\tilde{a}(T) = -\exp\left[-H_{\text{dS}} \sqrt{b^2 + T^2}\right], \quad (\text{A10})$$

which displays a nonsingular bounce behavior at $T = 0$ for $b \neq 0$. Incidentally, a similar bounce solution occurs if the initial condition $\tilde{a}(T_{\text{start}}) > 0$ is used: the corresponding solution is then given by (A10) with a plus sign in front of the exponential function on the right-hand side. Other bounce solutions, with

$$\tilde{a}(T) = \mp \exp \left[H_{\text{dS}} \sqrt{b^2 + T^2} - 2 H_{\text{dS}} \sqrt{b^2 + (T_{\text{start}})^2} \right], \quad (\text{A11})$$

may be more relevant for cosmology, as $\tilde{a}^2(T) \rightarrow \infty$ for $|T| \rightarrow \infty$.

The different solutions (A9) and (A10) make clear that the corresponding metrics (3.1) and (2.1) are essentially different. For both spacetime metrics, the Cauchy problem [3] and the foliation dependence or independence [11, 12] deserve further study.

Appendix B: Comparison with loop quantum cosmology and string cosmology

In this appendix, we review the bounce of the cosmic scale factor obtained from loop quantum cosmology (LQC) and compare with the bounce obtained from extended general relativity with the degenerate metric (3.1). For the record, we also compare with the bounce of string cosmology (SC). We set $c = 1$ and $\hbar = 1$, but keep G_N explicit.

As shown in Appendix B 1 of Ref [13] (and discussed in later reviews [14, 15]), the LQC bounce can be described by an *effective* Friedmann equation,

$$\left(\frac{\dot{a}}{a} \right)^2 = \frac{8\pi G_N}{3} \rho \left(1 - \frac{\rho}{\rho_B} \right), \quad (\text{B1a})$$

$$\rho_B = c_B (E_{\text{Planck}})^4, \quad (\text{B1b})$$

$$E_{\text{Planck}} \equiv 1/\sqrt{G_N} \approx 1.22 \times 10^{19} \text{ GeV}, \quad (\text{B1c})$$

$$l_{\text{Planck}} \equiv 1/E_{\text{Planck}} \approx 1.62 \times 10^{-35} \text{ m}, \quad (\text{B1d})$$

where the overdot stands for the derivative with respect to the cosmic time coordinate $t \in \mathbb{R}$. The dimensionless constant c_B in (B1b) is positive and, most likely, of order unity. In physical terms [14, 15], the value of ρ_B is set by the area gap $\Delta \sim (l_{\text{Planck}})^2$, $\rho_B \sim 1/\Delta^2$. Let us have a quick look at two domains of this bouncing cosmology, far away from the bounce and close to it.

For energy densities $\rho \ll \rho_B$ (or cosmic scale factors $a \gg a_B \equiv 1$), the effective Friedmann equation (B1) can be rewritten as

$$\left[1 + \frac{3}{8\pi G_N} \frac{1}{\rho_B} \left(\frac{\dot{a}}{a} \right)^2 \right] \left(\frac{\dot{a}}{a} \right)^2 \sim \frac{8\pi G_N}{3} \rho. \quad (\text{B2})$$

The structure of (B2) is the same as the one of our modified Friedmann equation (3.4c) with $a^2/[a - a_B]^2 \sim 1$. This allows for the following tentative identification

$$\frac{b^2}{4} \stackrel{\text{LQC?}}{\sim} \frac{3}{8\pi G_N} \frac{1}{\rho_B} = \frac{3}{8\pi} \frac{(E_{\text{Planck}})^2}{\rho_B}, \quad (\text{B3})$$

so that b would be of the order of l_{Planck} , as long as c_B from (B1b) is of order unity.

For energy densities ρ close to ρ_B , it is possible to use a series *Ansatz*,

$$a(t) = 1 + \hat{a}_2 t^2 + \dots, \quad (\text{B4a})$$

$$\rho(t) = \rho_B + \hat{r}_2 t^2 + \dots, \quad (\text{B4b})$$

with $\rho_B > 0$ and $\hat{r}_2 < 0$. Inserting (B4) into (B1a) gives

$$(\hat{a}_2)^2 = -\frac{2\pi G_N}{3} \hat{r}_2. \quad (\text{B5})$$

The quadratic coefficient \hat{a}_2 from (B5) has no direct dependence on ρ_B , which is given by fundamental constants according to (B1b). This result differs from what has been obtained from the degenerate-metric bounce, where the quadratic coefficient (4.4a) depends on $\sqrt{r_0}$, with $r_0 = 8\pi G_N \rho_B$ being a free parameter. A further difference is that, for the case of relativistic matter ($P = \rho/3$), the Ricci curvature scalar at the moment of the bounce does not vanish in the LQC calculation, according to Eq. (5.13) of Ref. [14], whereas it does vanish in the extended-general-relativity calculation, according to (4.9a) of Sec. IV A.

The conclusion is that the degenerate metric (3.1) may give a reasonable approximation of the LQC-bounce behavior at relatively low energy densities but not of the LQC-bounce dynamics close to the maximum energy density. At this moment, it is not clear which of the two models, extended general relativity with an appropriate degenerate metric or the effective theory from loop quantum cosmology, best describes the cosmic bounce, assuming such a bounce to be relevant to our Universe.

But another possibility is that the degenerate-metric bounce results from an entirely new phase [16] of string theory; see, e.g., Ref. [17] for a further review. For a direct comparison, we refer to two recent string-cosmology calculations [18, 19].

The authors of Ref. [19] obtained an explicit nonperturbative solution of the reduced equations of motion, assuming certain higher-order coefficients c_k , for $k \geq 3$, in the effective one-dimensional action of Ref. [18]. Specifically, the Hubble parameter $H_+^E(t)$ in the Einstein frame, for spatial dimensionality $d = 3$, is given by Eq. (3.24) in Ref. [19] and has the

following structure:

$$H_+^E(t) \sim \frac{t - t_{B,+}}{\alpha'/6 + t^2}, \quad (\text{B6a})$$

$$t_{B,+} \sim -\sqrt{\alpha'}, \quad (\text{B6b})$$

where $\alpha' > 0$ is the Regge slope related to the inverse of the string tension and $t_{B,+}$ the moment of the bounce [the other solution $H_-^E(t)$ is also given by (B6a), but with $t_{B,+}$ replaced by $t_{B,-} \sim \sqrt{\alpha'}$]. The Hubble parameter $H_+^E(t)$ is shown in Fig. 4 of Ref. [19] and resembles qualitatively the Hubble parameter obtained from the degenerate metric (3.1), as shown by the mid-right panels in Figs. 1 and 2.

Comparing the generic degenerate-metric result $H(t) \sim t/(b^2 + t^2)$ from Ref. [4] with (B6a) we have the following tentative identification:

$$b^2 \stackrel{\text{SC?}}{\sim} \frac{1}{6} \alpha', \quad (\text{B7})$$

which may be of order $(l_{\text{Planck}})^2$. Still, it needs to be emphasized that the existing string-cosmology calculations (just as the existing loop-quantum-cosmology calculations) are only indicative and that a possible string-theory phase replacing the big bang singularity may have highly unusual properties [16].

-
- [1] A.A. Friedmann, “Über die Krümmung des Raumes” (On the curvature of space), *Z. Phys.* **10**, 377 (1922); “Über die Möglichkeit einer Welt mit konstanter negativer Krümmung des Raumes” (On the possibility of a world with constant negative curvature), *Z. Phys.* **21**, 326 (1924).
 - [2] S. Weinberg, *Gravitation and Cosmology : Principles and Applications of the General Theory of Relativity* (John Wiley and Sons, New York, 1972).
 - [3] S.W. Hawking and G.F.R. Ellis, *The Large Scale Structure of Space-Time* (Cambridge University Press, Cambridge, England, 1973).
 - [4] F.R. Klinkhamer, “Regularized big bang singularity,” *Phys. Rev. D* **100**, 023536 (2019), arXiv:1903.10450.
 - [5] F.R. Klinkhamer, “On a soliton-type spacetime defect,” *J. Phys. Conf. Ser.* **1275**, 012012 (2019), arXiv:1811.01078.
 - [6] F.R. Klinkhamer and F. Sorba, “Comparison of spacetime defects which are homeomorphic but not diffeomorphic,” *J. Math. Phys. (N.Y.)* **55**, 112503 (2014), arXiv:1404.2901.

- [7] F.R. Klinkhamer and Z.L. Wang, “Nonsingular bouncing cosmology from general relativity,” *Phys. Rev. D* **100**, 083534 (2019), arXiv:1904.09961.
- [8] F.R. Klinkhamer and Z.L. Wang, “Asymmetric nonsingular bounce from a dynamic scalar field,” *Lett. High Energy Phys.* **3**, 9 (2019), arXiv:1906.04708.
- [9] F.R. Klinkhamer and Z.L. Wang, “Nonsingular bouncing cosmology from general relativity: Scalar metric perturbations,” to appear in *Phys. Rev. D*, arXiv:1911.06173.
- [10] A. Ijjas and P.J. Steinhardt, “Bouncing cosmology made simple,” *Class. Quant. Grav.* **35**, 135004 (2018), arXiv:1803.01961.
- [11] C. Teitelboim, “How commutators of constraints reflect the space-time structure,” *Annals Phys. (N.Y.)* **79**, 542 (1973).
- [12] S.A. Hojman, K. Kuchar, and C. Teitelboim, “Geometrodynamics regained,” *Annals Phys. (N.Y.)* **96**, 88 (1976).
- [13] A. Ashtekar, T. Pawłowski, and P. Singh, “Quantum nature of the big bang: Improved dynamics,” *Phys. Rev. D* **74**, 084003 (2006), arXiv:gr-qc/0607039.
- [14] A. Ashtekar and P. Singh, “Loop quantum cosmology: A status report,” *Class. Quant. Grav.* **28**, 213001 (2011), arXiv:1108.0893.
- [15] A. Ashtekar and A. Barrau, “Loop quantum cosmology: From pre-inflationary dynamics to observations,” *Class. Quant. Grav.* **32**, 234001 (2015), arXiv:1504.07559.
- [16] E. Witten, “Singularities in string theory,” in: *Proceedings of the International Congress of Mathematicians, Beijing 2002* (World Scientific Publ., Singapore, 2002), Vol. 1, pp. 495–504, arXiv:hep-th/0212349.
- [17] S.R. Das, “String theory and cosmological singularities,” *Pramana* **69**, 93 (2007).
- [18] O. Hohm and B. Zwiebach, “Duality invariant cosmology to all orders in α' ,” *Phys. Rev. D* **100**, 126011 (2019), arXiv:1905.06963.
- [19] P. Wang, H. Wu, H. Yang, and S. Ying, “Non-singular string cosmology via α' corrections,” *J. High Energy Phys.* **1910**, 263 (2019), arXiv:1909.00830.
- [20] N. Pinto-Neto and J.C. Fabris, “Quantum cosmology from the de-Broglie-Bohm perspective,” *Class. Quant. Grav.* **30**, 143001 (2013), arXiv:1306.0820.